

AD 716470

PREPARATION AND PROPERTIES OF RARE-EARTH COMPOUNDS

Semi-Annual Technical Report  
(4 June 1970 to 4 December 1970)

December 31, 1970

by

V. E. Wood, K. C. Brog, A. E. Austin, J. F. Miller  
W. H. Jones, Jr., C. M. Verber, E. W. Collings, R. D. Baxter

Sponsored By

Advanced Research Projects Agency

Under

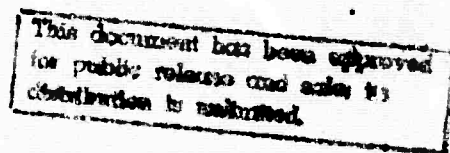
ARPA Order No. 1588  
PRON: W2-0-UX190-01-D1-DZ  
Contract No. DAAH01-70-C-1076

(Project Technical Director: V. E. Wood)

Reproduced by  
**NATIONAL TECHNICAL  
INFORMATION SERVICE**  
Springfield, Va. 22151

**BATTELLE MEMORIAL INSTITUTE**  
Columbus Laboratories  
505 King Avenue  
Columbus, Ohio 43201

Distribution of this document is Unlimited



**PREPARATION AND PROPERTIES OF RARE-EARTH COMPOUNDS**

**Semi-Annual Technical Report  
(4 June 1970 to 4 December 1970)**

**December 31, 1970**

**by**

**V. E. Wood, K. C. Brog, A. E. Austin, J. F. Miller  
W. H. Jones, Jr., C. M. Verber, E. W. Collings, R. D. ...**

**Sponsored By**

**Advanced Research Projects Agency**

**Under**

**ARPA Order No. 1588  
PRON: W2-O-UX190-01-D1-DZ  
Contract No. DAAH01-70-C-1076  
(Project Technical Director: V. E. Wood)**

**BATTELLE MEMORIAL INSTITUTE  
Columbus Laboratories  
505 King Avenue  
Columbus, Ohio 43201**

**Distribution of this Document is Unlimited**

## TABLE OF CONTENTS

|   | <u>page</u> |
|---|-------------|
| INTRODUCTION . . . . .  | 1           |
| MAGNETO FERROELECTRIC MATERIALS . . . . .                     | 2           |
| Introduction . . . . .  | 2           |
| Manganates . . . . .  | 3           |
| Molybdates . . . . .  | 18          |
| NARROW-GAP AND NARROW-BAND COMPOUNDS . . . . .                | 25          |
| PNICTIDES . . . . .   | 29          |
| NON-RADIATIVE ENERGY TRANSFER AMONG RARE-EARTH IONS . . . . . | 33          |
| REFERENCES . . . . .  | 36          |

## LIST OF TABLES

|   |   |
|---|---|
| TABLE I. DATA ON THE PREPARATION OF RARE-EARTH MANGANATES . . . . .   | 4 |
| TABLE II. OPTICAL-EMISSION SPECTROGRAPHIC ANALYSIS OF YTTRIUM<br>MANGANATE AND SOURCES OF MANGANESE . . . . . | 6 |
| TABLE III. CRYSTAL STRUCTURE DATA ON RARE-EARTH MANGANATES, UNIT CELL<br>PARAMETERS IN ANGSTROMS . . . . .    | 7 |

## LIST OF FIGURES

|  |    |
|--|----|
| FIGURE 1. MAGNETIC SUSCEPTIBILITY OF ORTHORHOMBIC $\text{YMnO}_3$ . . . . .  | 11 |
| FIGURE 2. MAGNETIC SUSCEPTIBILITY OF ORTHORHOMBIC $\text{HoMnO}_3$ . . . . .   | 13 |
| FIGURE 3. MAGNETIC SUSCEPTIBILITY OF ORTHORHOMBIC $\text{YbMnO}_3$ (78-322 K) . . . . .  | 15 |
| FIGURE 4. MAGNETIC SUSCEPTIBILITY OF ORTHORHOMBIC $\text{YbMnO}_3$ (4.2-322 K) . . . . .   | 16 |
| FIGURE 5. SCHEMATIC DIAGRAM OF THE PIEZOELECTRIC-RESONANCE DETECTOR . . . . .  | 22 |
| FIGURE 6. OSCILLOSCOPE DISPLAY OF A PIEZOELECTRIC-RESONANCE IN<br>SINGLE CRYSTAL $\text{Gd}_2(\text{MoO}_4)_3$ AT 15 MHZ . . . . . | 23 |
| FIGURE 7. PARTIAL ENERGY LEVEL DIAGRAM OF $\text{Ho}^{3+}$ IN $\text{CaF}_2$ . . . . .   | 34 |

## RESEARCH SUMMARY

Research has been performed to investigate potentially useful properties of rare-earth materials. This work has included studies in the areas of magnetoferroelectricity, narrow-band and narrow-gap compounds, rare-earth pnictides, and cooperative fluorescence of rare-earth ions in crystals. Manganates of Dy, Y, Ho, and Yb (including high-pressure orthorhombic phases of the last three) and molybdates of Eu, Gd, and Tb have been prepared and their electrical and magnetic properties studied. Although some of these compounds have interesting magnetic transitions, none appears to be even weakly ferromagnetic above about 10 K and hence they are not particularly attractive as ferromagnetoferroelectrics (materials having simultaneously ferroelectric and ferromagnetic properties). Electrical properties of these materials are discussed in the report; work on related compounds and on crystal growth is continuing. Electron paramagnetic resonance studies of the gradual low-temperature semiconductor-to-metal transition in  $\text{SmB}_6$  show a resonance which tentatively has been attributed to an excited state of  $\text{Sm}^{2+}$ . Transport measurements on a recently prepared high-purity, rf-melted sample of  $\text{SmB}_6$  will be made shortly. Results of both studies should provide insight into the conduction mechanism and the nature of the transition in such materials. Though recently reported research indicates that all rare-earth monopnictides ( $(\text{RE})\text{Pn}$ :  $\text{Pn} = \text{N}, \text{P}, \text{As}, \text{Sb}, \text{or Bi}$  with NaCl structure) are metallic, this may be due to intrinsic non-stoichiometry, and the question of whether the nitrides, in particular, are "really" metallic or semiconducting must still be considered open. Samples of  $\text{GdN}$  have been prepared and nuclear magnetic resonance studies will be used to determine the role of defects and to try to elucidate the electronic character. Finally, studies on the two-photon infrared-excited red fluorescence of  $\text{Ho}^{3+}$  ions in  $\text{CaF}_2$  have established that the fluorescence arises from cooperative energy transfer between  $\text{Ho}^{3+}$  ions rather than from successive excitation of a single ion. Work is continuing to determine the exact mechanism of the cooperative process.

**BLANK PAGE**

## INTRODUCTION

This program is concerned with the preparation, characterization, and measurement of electronic, magnetic, and optical properties of a number of classes of rare-earth compounds which possess certain combinations of physical properties of possible technological importance. The areas in which investigations are being conducted are:

- 1) Magnetoferroelectric materials
- 2) Narrow-band and narrow-gap materials
- 3) Rare-earth pnictides, and
- 4) Interactions of rare-earth ions in insulators.

Our original thought in proposing research in these areas was that in each of them insufficient systematic research was being conducted to assess accurately their potentialities. Recent research trends have altered this viewpoint to some extent and have caused and are continuing to cause some modifications in our research plans; considerable further work in all these areas is desirable, but priorities naturally need frequent re-examination. We shall discuss each of the above areas of research in turn. Each section will contain, as appropriate, an explanatory introduction, a discussion of materials preparation and characterization, a discussion of experimental results and their interpretation, and a summary of conclusions and plans for future work. It should become apparent that despite the diversity of the research areas, our work in them is connected in many ways by the distinctive physical and chemical properties of the rare earths.

## MAGNETO FERROELECTRIC MATERIALS

### Introduction

There are two classes of physical phenomenon which might be described by the term "magnetoelectric".<sup>1,2</sup> The first is the simultaneous existence in a solid of magnetic ordering and spontaneous electrical polarization. This phenomenon, which is the one of predominant interest in the present program, is usually called magnetoferroelectricity, assuming the electrical polarization is ferroelectric rather than antiferroelectric, and sometimes ferromagneto-ferroelectricity when the spin ordering is at least weakly ferromagnetic. The other phenomenon, usually just called magnetoelectricity, is an induced effect involving a change in the electric polarization proportional to an external magnetic field and a change in the magnetization proportional to an applied electric field. This effect can occur in materials with certain types of magnetic ordering; spontaneous electrical polarization is not necessary, although in principle it is more likely to lead to large values of the magnetoelectric coupling coefficients.<sup>3</sup> In magnetoferroelectric materials with the appropriate symmetry, the magnetization and polarization may be coupled through the magnetoelectric effect, so that a reversal of one leads to a reversal or a diversion through a fixed angle of the other. Other things being equal, magnetoferroelectrics are a little more interesting than magnetoelectrics from the device standpoint. It seems more sensible to approach the problem of developing new magnetoferroelectric materials by discovering or introducing magnetic properties in known classes of ferroelectrics rather than the other way around, since so little is known of why things are ferroelectric. (One should consider the possibility, though, that a material might be ferroelectric in the magnetically ordered state but not otherwise.<sup>4</sup>)

There is no fundamental reason why classes of materials containing rare-earth ions should necessarily possess magnetoferroelectricity more frequently or more strongly than others, but several classes of materials that have been suggested as containing magnetoferroelectrics do involve the rare-earths and seem to have other interesting properties as well. The classes of materials selected for initial examination were the rare-earth manganates and molybdates.

It is a little difficult to treat these classes together; so we shall discuss them sequentially.

### Manganates

The light (through Dy) rare-earth manganates,  $(RE)MnO_3$ , are orthorhombic, weakly ferromagnetic at low temperatures,<sup>5</sup> and not ferroelectric. The manganates of Y and the heavy rare-earths are normally hexagonal and are ferroelectric<sup>6</sup> with very high transition temperatures (around 700 C). They are substantially antiferromagnetic at low temperature,<sup>5</sup> showing only weak ferromagnetism of the rare-earth ions at very low temperature (9 K for  $ErMnO_3$  (private communication from R. Pauthenet)). By application of high pressure and temperature, the hexagonal materials can be converted to an orthorhombic form.<sup>7</sup> One could guess that this form might show a weak ferromagnetism associated with the Mn lattice, such as occurs in the light rare-earth manganates. However, no measurements of physical properties other than lattice parameter appear to have been made on these materials. We have prepared polycrystalline samples and studied properties of both forms of Y, Ho, and Yb manganates and of orthorhombic  $DyMnO_3$ . The cations were selected to provide a range of ionic radii and magnetic moments.

### Preparation and Characterization

Rare-earth manganates in powder form were prepared by solid-state reaction.  $YMnO_3$  was prepared in two ways: (1) by reacting intimate mixtures of 99.9%  $Y_2O_3$  and  $MnO_2$ , and (2) by dissolving  $Y_2O_3$  and Mn metal in nitric acid solution, evaporating to dryness and reacting the coprecipitated material. The other three rare-earth manganates were prepared by reacting intimate mixtures of 99.9% pure rare-earth oxide and  $MnO_2$ . Platinum containers were used for the high-temperature reactions. Mn and  $MnO_2$  purity is discussed below.

Data on some of the oxide reactions are given in Table I. The data indicate that single phase rare-earth manganates can be prepared by direct reaction of the oxides at moderate temperatures (in the range 1180 C to 1300 C). If the temperature is higher, it is indicated that an  $Mn_3O_4$  phase may form (second preparation in Table I). In some cases, a rare-earth oxide minor phase



TABLE I. DATA ON THE PREPARATION OF  
RARE-EARTH MANGANATES

| <u>Reactants</u>                           | <u>Reaction Conditions</u>                           | <u>Detected in Product by X-ray<br/>Diffraction Analysis</u>       |
|--|--|--|
| $Y_2O_3 + MnO_2$                           | 1300 C in oxygen, 4 hrs.                             | $YMnO_3$ only  |
| $Y_2O_3 + MnO_2$<br>(refired)              | 1350 C in oxygen, 4 hrs.<br>1275 C in oxygen, 6 hrs. | $YMnO_3$ + minor $Mn_3O_4$ phase<br>$YMnO_3$ only                  |
| $(Y_2O_3 + Mn)$ in $HNO_3$                 | Dried 125 C, 1250 C in air, 1 hr                     | $YMnO_3$ + trace unidentified phase                                |
| $Y_2O_3 + MnO_2$                           | 1250 to 1300 C in oxygen 3 hrs.                      | $YMnO_3$ *   |
| $Dy_2O_3 + MnO_2$                          | 1180 C in oxygen, 5 hrs.                             | $DyMnO_3$ only   |
| $Ho_2O_3 + MnO_2$<br>above + 1 wt% $MnO_2$ | 1350 C in oxygen, 5 hrs.<br>1280 C in oxygen, 5 hrs. | $HoMnO_3$ + minor $Ho_2O_3$ phase<br>$HoMnO_3$ + trace $Ho_2O_3$ * |
| $Yb_2O_3 + MnO_2$<br>above + 1 wt% $MnO_2$ | 1350 C in oxygen, 5 hrs.<br>1280 C in oxygen, 5 hrs. | $YbMnO_3$ + minor $Yb_2O_3$ phase<br>$YbMnO_3$ + trace $Yb_2O_3$ * |

\* Sources of material used for high pressure transformation and for electric and magnetic measurements

has formed. The cause of its appearance and persistence has not been determined. However, the more recent of those results presented indicate that the rare-earth oxide phase can be eliminated by adjusting the manganese oxide concentration in the starting material.

To aid in interpretation of observed electrical and magnetic properties, several samples of  $\text{YMnO}_3$  were analyzed by the optical-emission spectrographic method. Samples of Mn metal and Mn oxides also were analyzed to evaluate these materials for potential use in future preparative work. The results, which are given in Table II, show significant concentrations of several impurities in the manganate samples: Al, Si, Ca, Co and Fe. X-ray data indicate that these impurities may be present in minor phases (e.g.,  $\text{YAlO}_3$ ). The analytical results suggest that the high Al and Si concentrations did not originate in either the  $\text{MnO}_2$  or the  $\text{Y}_2\text{O}_3$ . Contamination during processing is suspected, and all operations are being monitored carefully in follow-up preparations. The analyses of sources of Mn indicate that the Mn metal is, from the standpoint of purity, to be preferred over available MnO or  $\text{Mn}_2\text{O}_3$ ; so this is being used in subsequent preparations.

The preparations of  $\text{YMnO}_3$ ,  $\text{YbMnO}_3$ , and  $\text{HoMnO}_3$  made by the sintering reaction of the oxides were checked for phase by X-ray diffraction. The materials had the hexagonal rare-earth manganate structure. The unit cell parameters and volume per mole are given in Table III. The X-ray diffraction data could be indexed on a hexagonal unit cell with either hexagonal space group  $P6_3\text{cm}$  or trigonal space group  $P3c1$ . The structure parameters have been given for the hexagonal space group  $P6_3\text{cm}$ ,<sup>8</sup> but the crystal structure might also be that of the alternative space group. The distinction in crystal atomic parameters may be quite slight, but there are differences in allowed magnetic structure symmetry. The hexagonal space group  $P6_3\text{cm}$  is of point group  $6\text{mm}$ , which allows both antiferromagnetic groups  $P6'_3\text{c}'\text{m}$ ,  $P6'_3\text{cm}'$  and ferromagnetic group  $P6_3\text{c}'\text{m}'$ , while the trigonal space group  $P3c1$  is of point group  $3\text{m}$  for which the magnetic group  $P3c'1$  can be ferromagnetic. It should be noted that in both classes the net magnetic moment is parallel to the c axis, as is the polarization direction in the ferroelectric state.

The heavy rare-earth manganates can be transformed under high pressure from the normal hexagonal phase into a more dense orthorhombic phase.<sup>7</sup> The conditions for the transformation of  $\text{YMnO}_3$ ,  $\text{YbMnO}_3$  and  $\text{HoMnO}_3$  were investigated

TABLE II. RESULTS OF OPTICAL-EMISSION SPECTROGRAPHIC  
ANALYSIS OF YTTRIUM MANGANATE AND SOURCES  
OF MANGANESE

|   | <u>Concentration of Impurity Element, wt %</u> |          |           |           |           |           |           |           |           |           |           |
|---|--|----------|-----------|-----------|-----------|-----------|-----------|-----------|-----------|-----------|-----------|
| <u>Material</u>                               | <u>Fe</u>                                      | <u>B</u> | <u>Si</u> | <u>Mg</u> | <u>Cu</u> | <u>Ni</u> | <u>Al</u> | <u>Co</u> | <u>Ca</u> | <u>Cr</u> | <u>Ba</u> |
| YMnO <sub>3</sub> (from<br>Mn metal)          | .1   | <.001    | 0.03      | <.001     | .001      | .003      | .001      | .005      | .007      | .01       |           |
| YMnO <sub>3</sub> (from<br>MnO <sub>2</sub> ) | .03  | <.001    | .1        | <.001     | .002      | .005      | 1.        | .01       | .02       | <.001     |           |
| Mn metal*                                     | <.001  | <.001    | <.001     | <.001     | <.001     | <.001     | <.002     | <.001     | .001      | <.003     | <.001     |
| MnO <sub>2</sub>                              | .1   | <.001    | <.001     | <.001     | <.001     | .003      | <.002     | <.001     | <.001     | .01       | <.001     |
| Mn <sub>2</sub> O <sub>3</sub>                | .2   | <.001    | .08       | .003      | .002      | .003      | .02       | .001      | .02       | .003      | .007      |

\* New supply; not that used in the preparation of YMnO<sub>3</sub>

TABLE III. CRYSTAL STRUCTURE DATA ON RARE-EARTH MANGANATES,  
UNIT CELL PARAMETERS IN ANGSTROMS\*

| Cpd.               | Hexagonal |       |          | Orthorhombic |       |       |               |
|--------------------|-----------|-------|----------|--------------|-------|-------|---------------|
|                    | $a_o$     | $c_o$ | $\Omega$ | $a_o$        | $b_o$ | $c_o$ | $\Omega^{**}$ |
| YMnO <sub>3</sub>  | 6.12      | 11.39 | 61.6     | 5.24         | 5.84  | 7.36  | 56.3          |
| YbMnO <sub>3</sub> | 6.02      | 11.36 | 59.4     | 5.16         | 5.76  | 7.30  | 54.2          |
| HoMnO <sub>3</sub> | 6.13      | 11.43 | 62.0     | 5.28         | 5.82  | 7.34  | 56.3          |

\* Error = 0.01 Å.

\*\* Volume per formula unit (Å<sup>3</sup>)

using both girdle and piston-cylinder high-pressure devices.<sup>9</sup> Powders of the compounds were sealed in platinum and heated to 1000 C for 2 hours under pressures from 35 to 60 kbar. The specimens were quenched from 1000 C while kept under high pressure. The  $\text{YMnO}_3$  and  $\text{HoMnO}_3$  were transformed completely at pressures greater than 35 kbar. The  $\text{YbMnO}_3$  required a pressure of 40 kbar at 1000 C for transformation. The specimens were produced in the form of sintered discs, 2-3 mm diameter. The hexagonal phase of  $\text{YbMnO}_3$  was also compressed into sintered discs at 1000 C under 35 kbar pressure.

The X-ray diffraction data of the high-pressure phases are indexable on orthorhombic unit cells (Table III). The possible space groups are centrosymmetric  $\text{Pbnm}$  and noncentrosymmetric  $\text{Pbn}2_1$ . Thus the crystal structure is similar to the rare-earth orthoferrites, orthochromites and light rare-earth manganates. It should be noted that physical property tests for acentricity are needed on each compound of these types. There is a volume decrease of about 9 percent in the transformation from the hexagonal to orthorhombic phase. This is in part the increase in cation-oxygen coordination, with that of manganese going from 5 to 6 oxygens and that of the rare earth going from 7 to 12.

Single crystals of the  $\text{YMnO}_3$ -type compounds have been grown previously from molten fluxes of lead and bismuth oxides. In this method there is always some question of impurities in solid solution and of trapped inclusions. An alternative method of crystal growth was sought which might also permit growth of oriented thin films suitable for optical transmission measurements. Chemical vapor deposition appeared to be suitable for growth of  $\text{YMnO}_3$  crystals free of the impurities encountered in the flux method and also for deposition of thin films. The process is similar to that employed for growth of ferrites and garnets.<sup>10</sup>

Various vapor-phase reactions that could be used for growth of rare-earth manganates were evaluated thermodynamically. Favorable processes were:

- 1) Growth of rare-earth manganates by hydrolysis of the rare-earth and manganese chlorides in a continuous flow system.

- 2) Deposition of rare-earth manganate by decomposition and oxidation of the rare-earth and manganese acetylacetonates in a continuous flow system.
- 3) Regrowth of the rare-earth manganate by chloride vapor phase transport through a temperature gradient with a HCl atmosphere in a sealed tube.

Experiments on vapor transport through HCl were first tried with source material of  $\text{YMnO}_3$  powder. Thermodynamic calculations for vapor transport<sup>11</sup> show that there is no dependence of the free energies of reaction on HCl pressure and that the hot and cold temperatures respectively should be above and below about 1000 C. Accordingly, experiments were tried using a source of  $\text{YMnO}_3$  powder at 1025 C under 0.2 atmosphere HCl in a sealed silica tube. Crystals of  $\text{Mn}_3\text{O}_4$  and possibly  $\text{Y}_2\text{O}_3$  were deposited in the cold end at 810 C. However, there was also some silica reaction with the HCl and deposition of some silicate phases. Because of these side reactions in the closed system, the experiments were directed to the first reaction using an open tube continuous-flow system for oxidation of  $\text{YCl}_3$  and  $\text{MnCl}_2$  vapors of  $\text{H}_2\text{O}$ . With this method, the corrosive HCl gas should be swept away by the carrier gas. The initial experiments yielded deposits of  $\text{Y}_2\text{O}_3$  at 1000 to 1025 C. Increased temperature and oxygen pressure apparently are needed for reaction of the  $\text{MnCl}_2$  vapor. Further experiments will be made with wet oxygen and substrates heated locally to 1200 C to control the deposition reaction.

#### Magnetic Measurements

The magnetic susceptibilities of the hexagonal Y, Ho, and Yb manganates and of  $\text{DyMnO}_3$  were measured in the range 77 - 300 K. The results agreed extremely well with those of Pauthenet;<sup>5</sup> so there seemed to be little point in giving any high priority to the extension of the measurements to helium temperatures. Next we discuss separately our results for orthorhombic  $\text{YMnO}_3$ ,  $\text{YbMnO}_3$  and  $\text{HoMnO}_3$  and compare them to those for the corresponding hexagonal phase materials.

The magnetic susceptibility of orthorhombic  $\text{YMnO}_3$  over the temperature range 4.2 - 559 K is shown in Fig. 1 where it is clear that there are two interesting temperature regimes. Over the range 78 - 559 K the susceptibility obeys

a Curie-Weiss law,  $\chi = C/(T - \theta)$ , with a negative  $\theta$  and there is no field dependence of the susceptibility. Below about 40 K there is an onset of weak ferromagnetism as exhibited by the discrepancy between the measured  $\chi$  values at two field strengths (9.88 and 5.82 kOe).

To analyze the data, we make the reasonable assumption that the specimen consists of  $\text{YMnO}_3$  contaminated with  $\text{Mn}_3\text{O}_4$ , which seems to be invariably present in small amounts in preparations of  $\text{YMnO}_3$ . According to the most recent information,<sup>12</sup> the Curie temperature of  $\text{Mn}_3\text{O}_4$  is 46 K. This agrees very well with the temperature below which the susceptibility shows a field dependence (Fig. 1). Using published data<sup>13</sup> on the magnetic properties of ferrimagnetic  $\text{Mn}_3\text{O}_4$ , we may calculate the fraction of this impurity which is present in the specimen.

Below the Curie temperature of the ferrimagnetic contaminant the susceptibility may be written as:

$$\chi_1 = \chi_\infty + \frac{c\sigma}{H_1} \quad , \quad (1)$$

where  $\chi_1$  = susceptibility measured at field  $H_1$

$\chi_\infty$  = susceptibility extrapolated to infinite field

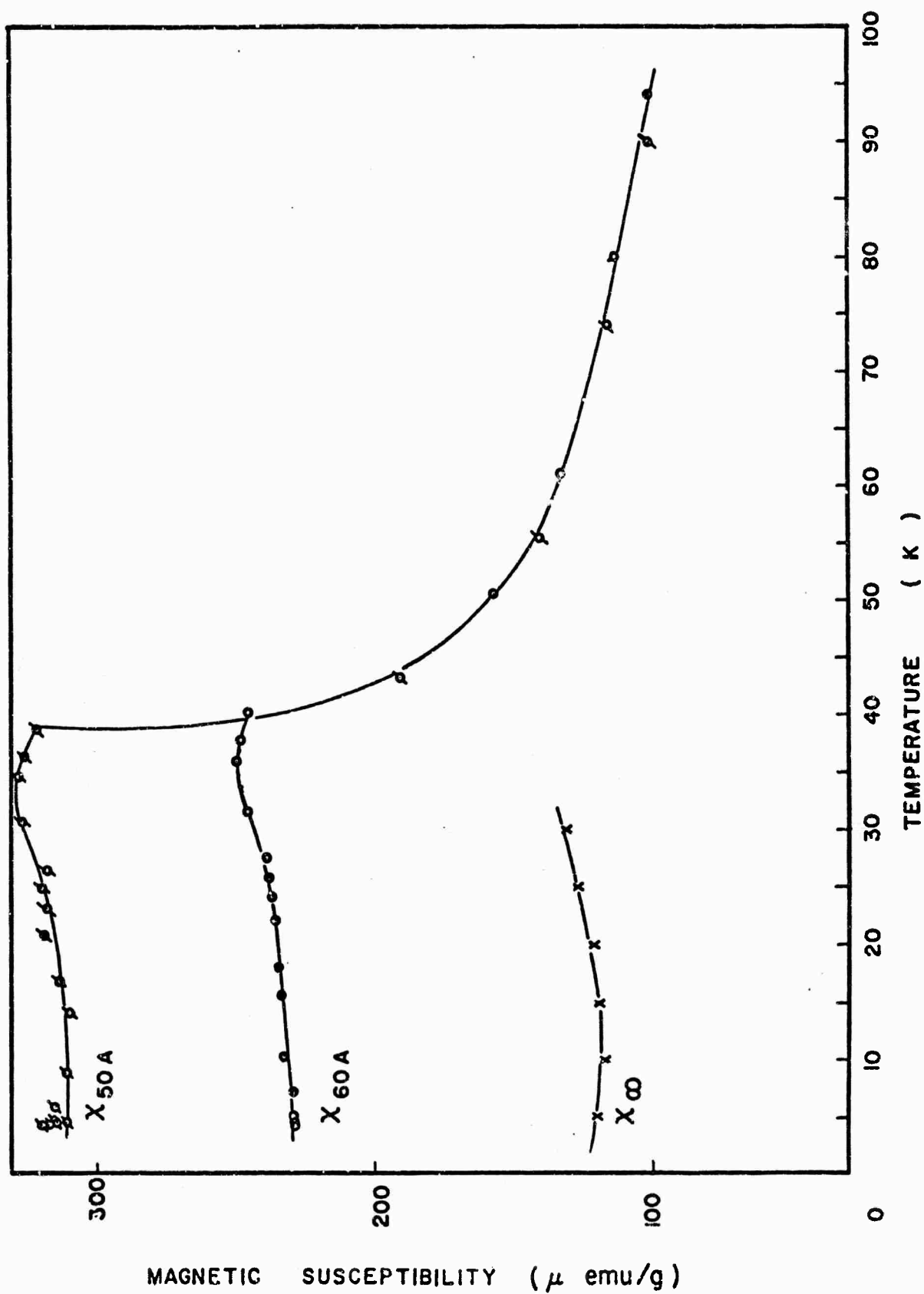
$\sigma$  = saturation magnetization\* of the ferrimagnetic contaminant  
of concentration  $c$ .

---

\* (1.7 Bohr magnetons per molecule of  $\text{Mn}_3\text{O}_4$ )

From the data of Fig. 1 we find  $c = 2.6$  wt percent. Below the Curie temperature of  $\text{Mn}_3\text{O}_4$  the susceptibility of  $\text{YMnO}_3$  is correctly represented by  $\chi_\infty$  and is thus directly measured. Above the Curie point of  $\text{Mn}_3\text{O}_4$ , the susceptibility of  $\text{YMnO}_3$  must be determined from the experimental value by correcting for the paramagnetism of the  $\text{Mn}_3\text{O}_4$  impurity. This can be done either by using the moment per Mn ion determined in the ordered state or using direct susceptibility vs temperature measurements of pure  $\text{Mn}_3\text{O}_4$ . However, the lack of knowledge of the spin order prevents knowledge of the former and no data were available for the latter. In any case, with such a small concentration of  $\text{Mn}_3\text{O}_4$ , it is satisfactory to use an estimated value of the moment per Mn to correct the

FIGURE 1. MAGNETIC SUSCEPTIBILITY OF ORTHORHOMBIC  $\text{YbO}_3$  AS A FUNCTION OF TEMPERATURE AND APPLIED MAGNETIC FIELD;  $\circ$ -9.88 kOe,  $\phi$ -5.82 kOe,  $\times$ -SUSCEPTIBILITY EXTRAPOLATED TO INFINITE FIELD





observed susceptibility to obtain the values characteristic of  $\text{YMnO}_3$ . Assuming an average moment of about 2 Bohr magnetons per Mn ion in  $\text{Mn}_3\text{O}_4$ , the susceptibility of orthorhombic  $\text{YMnO}_3$  is found to obey a Curie-Weiss law with a paramagnetic  $\theta$  value of about - 50 K and an effective magneton number of about 4.8. In addition, a cusp-like behavior characteristic of antiferromagnetic order is observable near 40 K. More refined analysis is in progress.

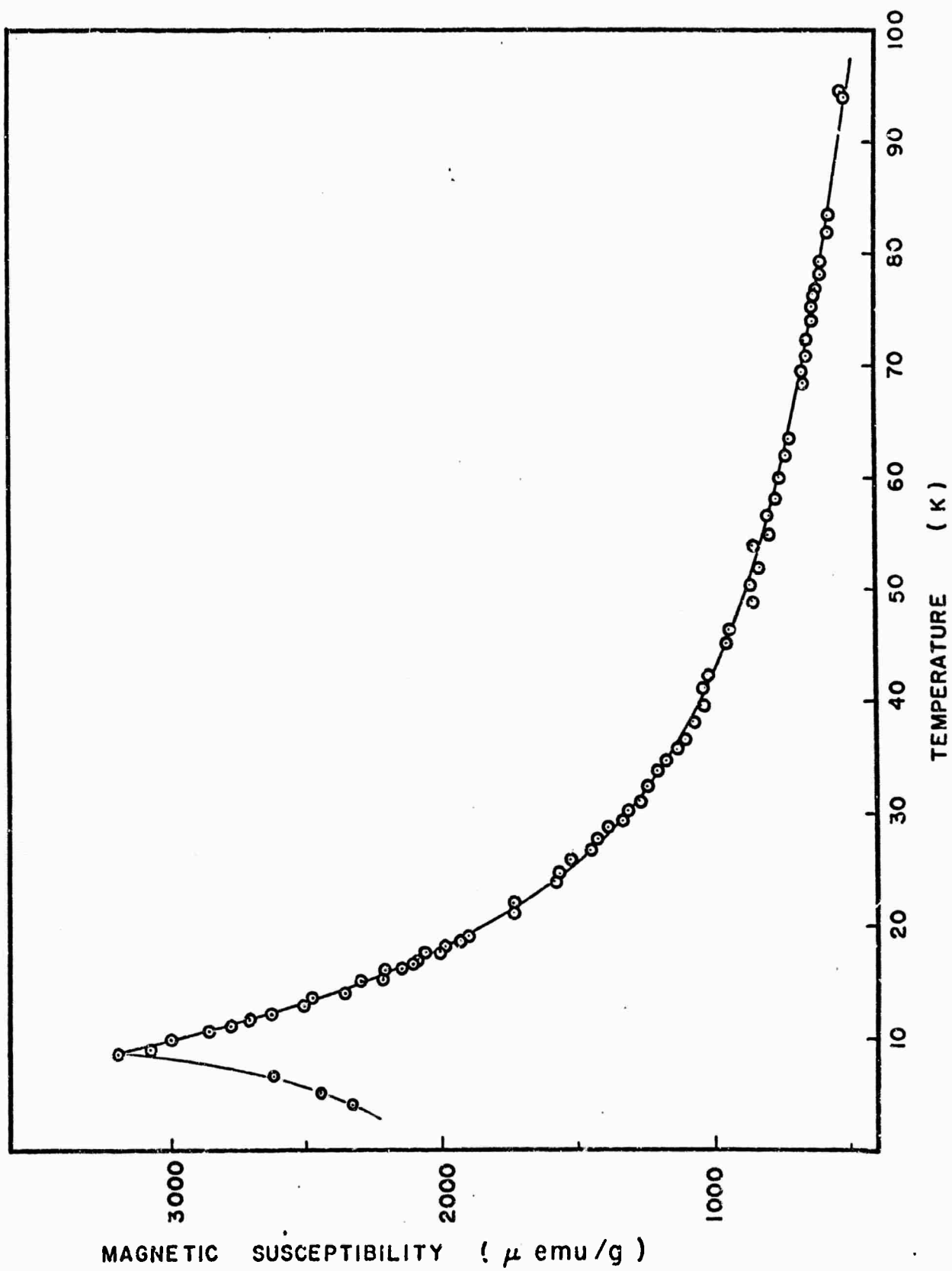
The magnetic susceptibility of orthorhombic  $\text{HoMnO}_3$  was measured over the temperature range 4.2 - 296 K. Below 40 K a small amount of ferromagnetic contamination was evident and at 8.5 K a sharp peak in the susceptibility was observed. As in the case of the  $\text{YMnO}_3$  sample we assume that the onset of weak ferromagnetism near 40 K is due to  $\text{Mn}_3\text{O}_4$ , and following the analysis given above we find it to have a concentration of about 1.5 weight percent. Above 40 K the paramagnetism of  $\text{Mn}_3\text{O}_4$  represents an insignificant fraction of the observed susceptibility because  $\chi(\text{HoMnO}_3) \gg \chi(\text{Mn}_3\text{O}_4)$ . Thus the contaminant operated principally as a diluent. The corrected susceptibility characteristic of orthorhombic  $\text{HoMnO}_3$  is shown in Fig. 2. The pronounced peak in the susceptibility of 8.5 K is typical of a transition from a paramagnetic to an antiferromagnetic regime. In the paramagnetic region the susceptibility can be fitted to a Curie-Weiss law of the form

$$\chi = \chi_0 + N p_{\text{eff}}^2 \beta^2 / (T + 5.5 \text{ K})$$

where  $N$  is the number of molecules,  $p_{\text{eff}}$  is the effective magneton number given by  $g\sqrt{S(S+1)}$  and  $\beta$  is the Bohr magneton. We find  $p_{\text{eff}} \approx 10$  and  $\chi_0 \sim 45 \mu\text{emu/gm}$ . The latter quantity is believed to result from orbital paramagnetism associated with the Ho ion. Assuming a value of  $p_{\text{Mn}}^2 \approx 23$  as determined for  $\text{YMnO}_3$ , we calculate  $p_{\text{Ho}} \approx 8.7$ . This is to be compared with the value of 10.6 expected for free  $\text{Ho}^{3+}$  ions.

The magnetic susceptibility of orthorhombic  $\text{YbMnO}_3$  was measured over the temperature range 4.2 - 322 K. The absence of any ferromagnetic contaminant was demonstrated by the absence of any field dependence of the susceptibility at any temperature. The data could not, however, be fitted with a single Curie-Weiss law over the entire temperature range because of excess paramagnetism at the lower temperatures.

FIGURE 2. MAGNETIC SUSCEPTIBILITY OF ORTHORHOMBIC  $\text{HoMnO}_3$  (DATA CORRECTED FOR EFFECT OF 1.5 wt PER CENT  $\text{Mn}_3\text{O}_4$ ) AS A FUNCTION OF TEMPERATURE



Over the temperature range 78 - 322 K the susceptibility does nearly obey a Curie-Weiss law with a paramagnetic  $\theta$  value of - 65 K and an effective moment of 6.5 Bohr magnetons per molecule. This is shown in Fig. 3 where we have plotted  $\chi$  as a function of  $1/(T + 65 \text{ K})$ . The  $\chi$  intercept of zero indicates the absence of temperature-independent contributions such as orbital paramagnetism, and suggests a simple Curie-Weiss behavior given by

$$\chi_1 = N p_{\text{eff}}^2 \beta^2 / (T + 65 \text{ K}) \quad , \quad \text{with } p_{\text{eff}} \approx 6.5 \quad .$$

The failure of this same equation to represent the observed susceptibility at temperatures below 70 K is shown in Fig. 4 where we extend the range of Fig. 3 to include the lower temperature data. The temperature dependence of this excess paramagnetism is found to obey a Curie-Weiss law given by  $\chi_2 = C_2 / (T + 3 \text{ K})$ . Having obtained these approximate solutions for the extreme temperature ranges it is possible to perform a self-consistent fit of all the data to two Curie-Weiss laws. The result is:

$$\chi = \frac{N p_{\text{eff}}^2 \beta^2}{T + 65 \text{ K}} + \frac{C_2}{T + 3 \text{ K}} \quad (2)$$

where now  $p_{\text{eff}} = 6.1$  per molecule.

It would seem that the first term in Eq. 2 represents the Mn spins while the second corresponds to the Yb spins. However, the effective moment value of 6.1 is much larger than that found for the Mn spins in the  $\text{YMnO}_3$  sample and thus must include contributions from the Yb spins. This implies that magnetic order within the Yb sublattice occurs almost simultaneously with the onset of antiferromagnetism among the Mn spins. Using the value of  $p_{\text{Mn}}^2 = 23$  found for the  $\text{YMnO}_3$  sample and assuming  $p_{\text{eff}}^2 = p_{\text{Yb}}^2 + p_{\text{Mn}}^2$  we find  $p_{\text{Yb}} = 3.7$ . This is to be compared with the value of 4.5 expected for trivalent Yb. We conclude that the second term in Eq. 2 results from impurities in our  $\text{YbMnO}_3$  sample. Further measurements at lower temperatures are being conducted to confirm this conclusion and the foregoing analysis.

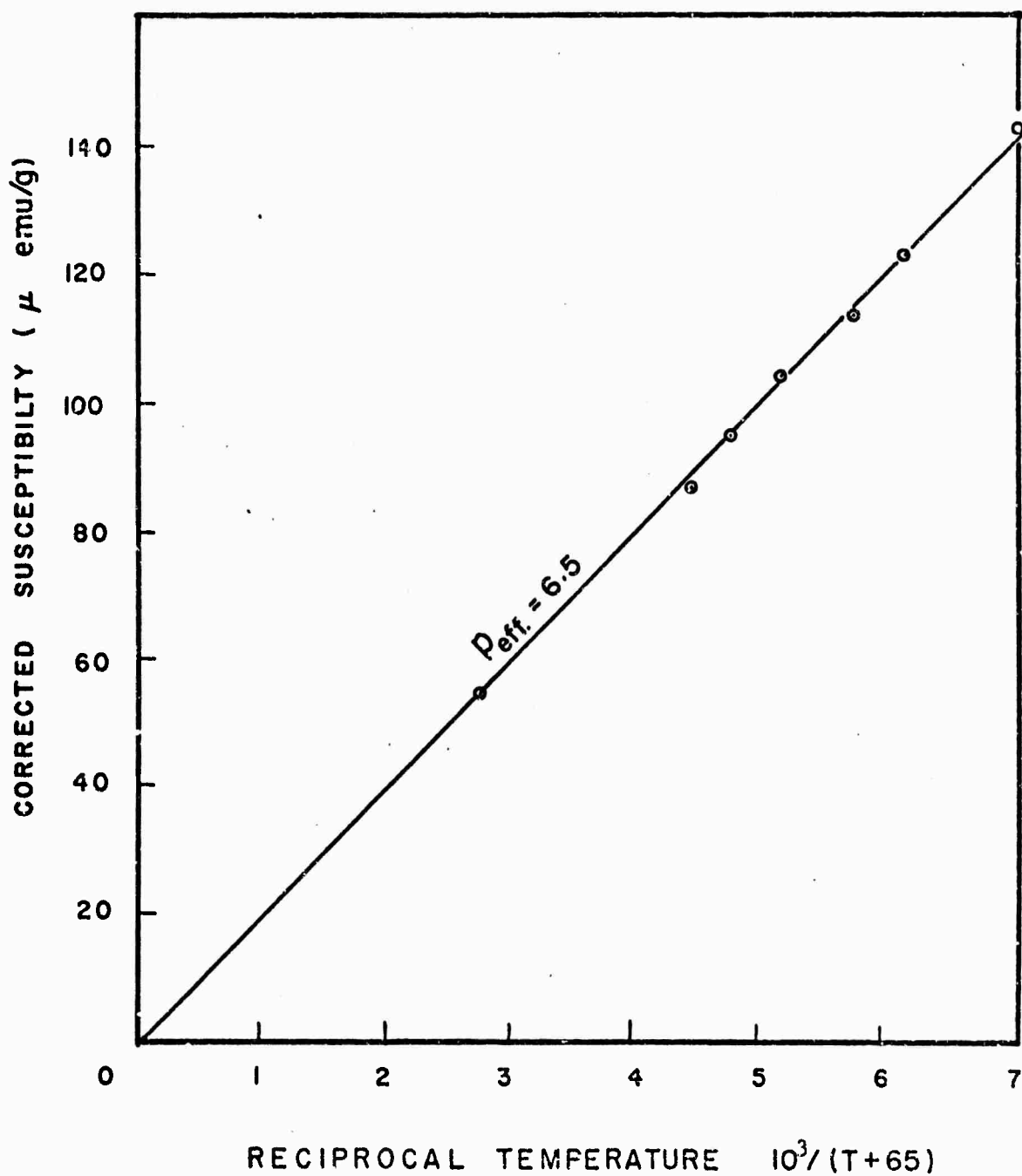


FIGURE 3. MAGNETIC SUSCEPTIBILITY OF ORTHO-RHOMBIC  $\text{YbMnO}_3$  AS A FUNCTION OF  $(T+65)^{-1}$  OVER THE TEMPERATURE RANGE 78 - 322K

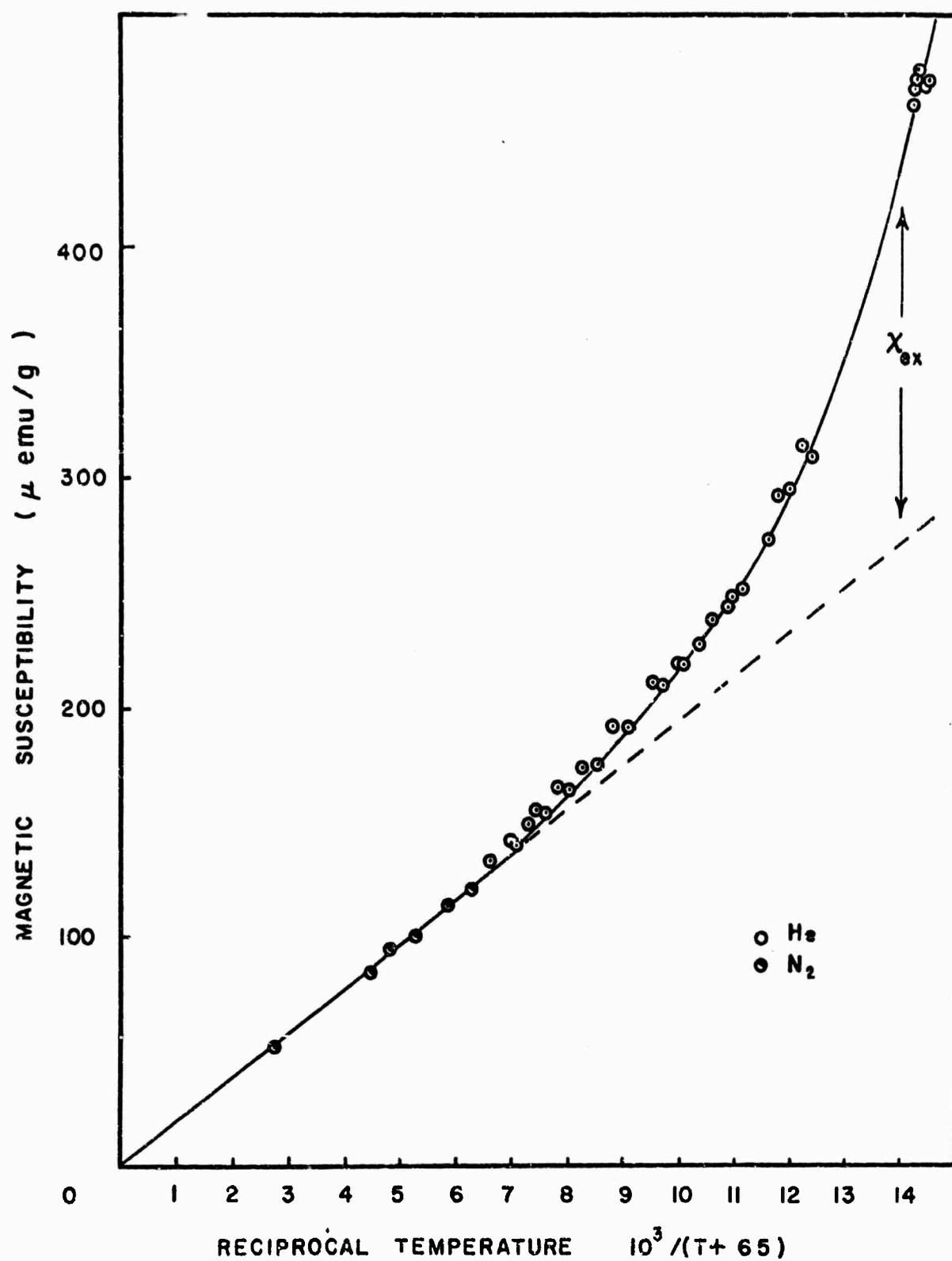


FIGURE 4. MAGNETIC SUSCEPTIBILITY OF ORTHORHOMBIC  $\text{YbMnO}_3$  AS A FUNCTION OF  $(T+65)^{-1}$  OVER THE TEMPERATURE RANGE OF 4.2 - 322K

## Ferroelectric Measurements

Another important question about the orthorhombic phase of rare-earth manganates is that of the existence of ferroelectricity. Such behavior can only exist in non-centrosymmetric crystals and as indicated previously the X-ray powder patterns do not allow one to state with certainty that the point symmetry is such that this phase is acentric. The simplest test for acentricity is the Wooster test for pyroelectricity. This test consists of loosely placing the sample on a metallic plate at room temperature and immersing the assembly in liquid nitrogen. If the sample is pyroelectric, the electric polarization will change with temperature causing a polarization charge to be built up on the surface. This in turn induces a charge of opposite sign on the metal plate and coulomb forces cause the sample to adhere to the plate. It was found that our orthorhombic-phase samples failed the Wooster test for pyroelectricity whereas the hexagonal-phase materials passed the test. Admittedly, the Wooster test is rather crude; however, these results show that the pyroelectric effect is at least significantly reduced under transformation to the orthorhombic phase. Dielectric constant and electrical conductivity measurements were also made on orthorhombic  $\text{YMnO}_3$  in order to detect the existence of ferroelectricity. Preliminary dielectric constant measurements made with a capacitance bridge operating at 1600 Hz indicated a very large value of order 1000. Subsequent frequency dependence measurements, however, suggested that these effects resulted from contact problems. These suspicions were confirmed by DC and pulse conductivity measurements where it was demonstrated that the fired silver-paste contact to the specimen formed a Schottky barrier in the interface region. The current-voltage relationship was found to obey an equation of the form  $i = i_0 (e^{eV/kT} - 1)$ . The result strongly indicates that the low frequency capacitance studies actually measured the contact capacitance. By extending the frequency range to 100 MHz we have determined that the dielectric constant of orthorhombic  $\text{YMnO}_3$  at 300 K is less than 3. DC electrical conductivity measurements using a 4 terminal technique to avoid contact difficulties have been made over the temperature range of 300 - 700 K. These showed p-type semiconducting behavior. There is a break in the conductivity - temperature curve at around 500 K. This might indicate a ferroelectric-paraelectric transition, but breaks not associated with such a transition do occur in the hexagonal

manganates<sup>14</sup> along with breaks at the ferroelectric Curie temperatures. A similar situation occurs in the lattice parameters.<sup>15</sup>

From our results and those in the literature, it appears that the hexagonal phases of the heavy rare-earth manganates are magnetoferroelectric only at very low temperatures ( $< 10$  K), while the orthorhombic phases investigated are antiferromagnetic and probably not ferroelectric, and thus not magnetoferroelectric. There are, however, a number of investigations on these and related materials which need to be carried out, some of which have already started. In view of reports of ferroelectricity in orthorhombic rare-earth chromites,<sup>16</sup> and since there are a number of interesting magnetic-ordering possibilities in materials with more than one kind of 3d-ion, it appears that a study of (RE)  $(\text{Mn}_{1-x}\text{Cr}_x)_2\text{O}_3$  compounds is desirable. In this work, synthesis will be made using higher purity starting materials, which should facilitate further electrical and optical measurements. We are considering measurements of second-harmonic generation in these materials, which could settle questions regarding acentricity as well as being of intrinsic interest.<sup>17</sup> We are also looking into direct measurements (on polycrystalline samples) of the magnetoelectric susceptibility.

### Molybdates

We now turn to the rare-earth molybdates of formula  $(\text{RE})_2(\text{MoO}_4)_3$ . In the metastable "beta" phase, these materials are ferroelectric<sup>18</sup> at temperatures below about 430 K. Inasmuch as they contain only rare-earth ions, one would not expect these compounds to order magnetically at very high temperatures, but one might anticipate being able to raise the ordering (Curie or Néel) temperature somewhat by introduction of 3d-ions, although extensive replacement does not seem favorable because of the smallness of these ions. We prepared  $\beta$ -phase Gd, Eu, and Tb molybdates in powder form to provide material to be used for magnetic susceptibility studies, for piezoelectric studies, and as starting material for crystal growth.

### Preparation and Characterization

For the initial studies, the molybdates were prepared in powder form by the direct reaction of intimate mixtures of 99.5% pure  $\text{MoO}_3$  and 99.9% pure rare-earth

oxides. (In the latter materials, the purity refers to the rare-earth content only; this is the usual basis for purity assay data among suppliers of rare-earth oxides). The compound was formed by firing this mixture, prepared by grinding the constituent oxides together, in air or in oxygen at 1100 C for 5 hours or more. In several cases, single-phase  $\text{Gd}_2(\text{MoO}_4)_3$  charges for crystal growth were prepared simply by fusing the oxide mixtures in a Pt crystal-growth crucible.

Small crystals of  $\text{Gd}_2(\text{MoO}_4)_3$  and  $\text{Tb}_2(\text{MoO}_4)_3$  were grown by the Czochralski (crystal pulling) technique. For the crystal-growth runs, the materials were contained in Pt or Pt90-Rh10 crucibles and were melted and held at the desired temperature by use of a 480 kHz rf generator with a feed-back loop from the output circuit to a fast-response current-adjusting control unit. Growth was initiated on platinum loops and pulls were made at rates in the range 1 to 2.5 cm per hour, with the growing crystal rotated at 60 rpm. Growths were made in both oxygen and air; no consistent significant difference attributable to the atmosphere was noted.

In the growth of  $\text{Gd}_2(\text{MoO}_4)_3$ , which was used as the pilot material, regions of dark material were sometimes obtained. No firm conclusion has been reached regarding the cause of the deposition of this material. Some possible causes are deviation from Gd/Mo stoichiometry, impurity effects, and oxygen deficiency. Nevertheless, the results indicate that transparent material can best be grown by using pre-reacted molybdate powder and by using low growth rates ( $\leq 1$  cm per hour).

Gadolinium molybdate,  $\text{Gd}_2(\text{MoO}_4)_3$ , was analyzed by X-ray diffraction on a powdered piece of single crystal. Cr K $\alpha$  radiation was used with a 114.8 mm diameter camera for dispersion of the X-ray diffraction pattern. The data could be indexed either on the pseudotetragonal unit cell  $a_0 = 10.414$  Å,  $c_0 = 10.696$  Å or on the orthorhombic unit cell  $a_0 = 10.386$  Å,  $b_0 = 10.419$  Å,  $c_0 = 10.700$  Å with an error of 0.005 Å. Varying breadths of overlapped reflections indicated the preference for the orthorhombic unit cell. These results are essentially in agreement with recent data of Keve et al.<sup>19</sup> The data of Drobyshev et al.<sup>20</sup> appear in reasonable agreement; however, according to their published data there may be a second phase of  $\text{Gd}_2\text{O}_3$  in their material. Analysis of the orthorhombic structure<sup>19</sup> indicates the transition from high temperature tetragonal  $\text{P}\bar{4}2_1\text{m}$  to low temperature  $\text{Pba}2$  involves slight displacement of Gd and O from mirror planes in  $\text{P}\bar{4}2_1\text{m}$ . Thus, conceivably by a shift of parameters with temperature, the transition might be



second order rather than first order. A note by Kvapil<sup>21</sup> indicating a doubled c-axis is probably incorrect since the diffraction lines they claim are indexable on the orthorhombic unit cell given above.

### Ferroelectric Measurements

As a routine test, preliminary pyroelectric (Wooster test) and piezoelectric-resonance (described later) measurements to confirm acentricity were made on powder specimens of each of the above molybdates and on one of the first of our crystals of  $\text{Gd}_2(\text{MoO}_4)_3$ . (Such measurements are desirable because the presumed space group  $\text{Pba2}$  is again a Buerger group.) All of these samples were found to be acentric by both techniques. The dielectric constant of the  $\text{Gd}_2(\text{MoO}_4)_3$  crystal, which was not of good optical quality, was measured with a Wayne-Kerr capacitance bridge over the temperature range 300 - 500 K to check the reported small dielectric constant anomaly at the ferroelectric transition temperature of 432 K.<sup>18</sup> This measurement could not be made in the most favorable manner because the crystal was cut such that the c-axis, along which the entire dielectric anomaly occurs, could not be made parallel to the electric field applied by the capacitor plates. After correcting for this misalignment, the observed change in the dielectric constant was about an order of magnitude smaller than that previously reported, indicating a high degree of strain in our material. This conclusion was further supported by the fact that an optical display of the ferroelectric domains, using crossed polarizers and a microscope, showed relatively few ferroelectric regions. Furthermore, the domains, which were randomly oriented and very small, could not be made to grow in the presence of a  $2 \times 10^4$  volt/cm polarizing field as the temperature was cycled through the transition region. To test the reliability of these experimental techniques a high-optical-quality single crystal of  $\text{Gd}_2(\text{MoO}_4)_3$  was purchased from Isomet, Inc. This crystal was in the form of a thin platelet with the c-axis perpendicular to the broad faces. Small ferroelectric domains were easily observable in polarized light below the ferroelectric Curie temperature while above this temperature the sample was uniformly clear. The application of a  $2 \times 10^4$  volt/cm polarizing field as the temperature was lowered through the transition region was sufficient to reduce the number of domains in the entire sample to 3. The dielectric constant anomaly at the ferroelectric transition was in good agreement with that reported in the literature.

Using the Isomet crystal, the feasibility of using piezoelectric resonance experiments to measure both piezoelectric coupling coefficients and polarization relaxation times in single crystals was demonstrated. In these types of experiments the sample is placed in a capacitor which forms part of the tank circuit of an RF oscillator which is frequency modulated in the audio range (Fig. 5). By virtue of the piezoelectric coupling, the applied RF electric field causes acoustic vibrations in the sample, and at mechanical resonances of the sample large changes in the RF level of oscillation are observed. After diode detection the audio signal is amplified and displayed on the y axis of an oscilloscope. Fig. 6 shows a typical resonance observed at about 15 MHz. The decaying oscillations, seen after passage through the resonance (large peak), result from beats between the decaying polarization and the applied electric field. The envelope of these oscillations provides a measure of the decay rate. In order to successfully measure the tensor components of the coupling coefficient and corresponding relaxation times in this way, it is necessary to study several single crystals cut in different orientations. In the case discussed here it is assumed that only the shear mode about the c-axis is excited since all other coupling coefficients are small in  $\text{Gd}_2(\text{MoO}_4)_3$ .

Some other studies of the phase transition to the ferroelectric state in  $\beta\text{-Gd}_2(\text{MoO}_4)_3$  were undertaken. The nature of this transition is of considerable interest at present since the ordered phase is ferroelastic as well as ferroelectric;<sup>18,22</sup> that is, there is a spontaneous strain which is reorientable by an external stress. Measurements of bulk magnetic susceptibility showed no anomaly at the transition temperature. The order of this phase transition has been the subject of much discussion;<sup>22</sup> application of the theory of phase transitions showed that there is nothing to prevent the transition from being second order; thermodynamic arguments are somewhat inconclusive. A short paper on this work has been prepared.

While this work was in progress, we received a preprint of the work of Keve et al.<sup>19</sup> in which they mention that they found no magnetic transitions in  $\beta\text{-Gd}_2(\text{MoO}_4)_3$  or  $\beta\text{-Tb}_2(\text{MoO}_4)_3$  down to 1.4 K. Their high-temperature paramagnetic moment for  $\text{Gd}_2(\text{MoO}_4)_3$  agrees well with ours. It is unlikely that a transition could be induced by adding other ions; thus it seems that the rare-earth molybdates of this type are not sufficiently interesting from the magnetoferroelectric

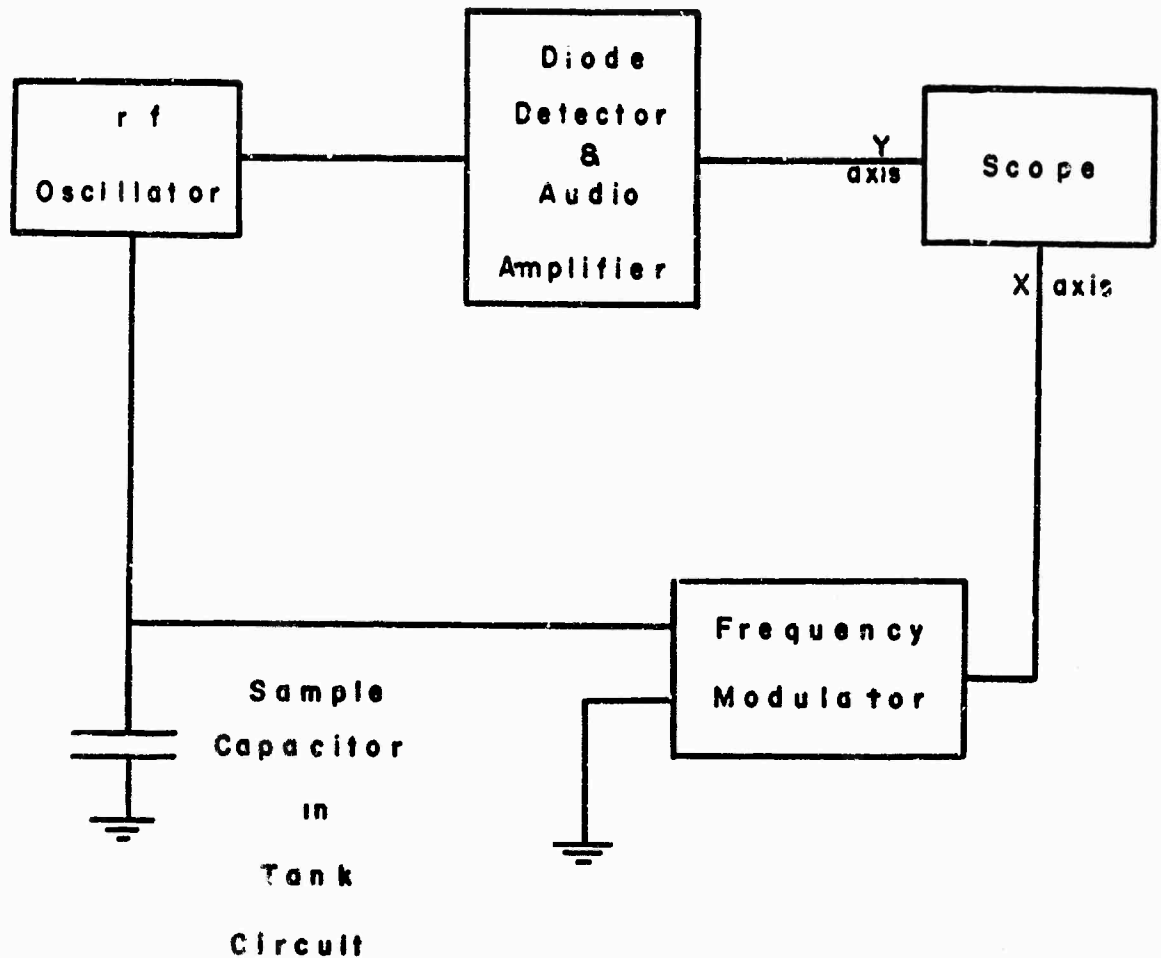


FIGURE 5. SCHEMATIC DIAGRAM OF THE PIEZOELECTRIC-RESONANCE DETECTOR. BOTH A MARGINAL OSCILLATOR AND A SUPER-REGENERATIVE OSCILLATOR HAVE BEEN USED. THE RESONANCE SIGNALS DISPLAYED ON THE SCOPE MAY BE ENHANCED BY A FACTOR OF 100 to 1000 BY USING CONVENTIONAL LOCK-IN DETECTION. THE LATTER APPARATUS IS NOT SHOWN.

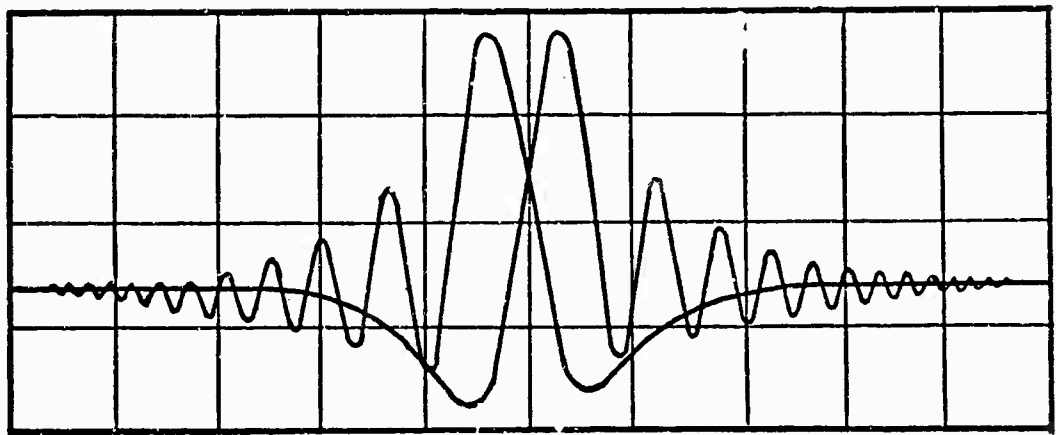


FIGURE 6. OSCILLOSCOPE DISPLAY OF A PIEZOELECTRIC-RESONANCE SIGNAL OBSERVED IN A SINGLE CRYSTAL OF  $\text{Gd}_2(\text{MoO}_4)_3$  AT 15 MHZ. THE X AXIS DEFLECTION IS PROPORTIONAL TO THE OSCILLATOR FREQUENCY WHICH IS MODULATED AT 60 HZ WITH AN AMPLITUDE OF ABOUT 10 KHZ. THE PATTERN IS A DUAL DISPLAY CORRESPONDING TO PASSAGE THROUGH RESONANCE (LARGE PEAK) FROM BOTH DIRECTIONS.

standpoint to justify further work on them. We have been giving some consideration to a number of other rare-earth molybdates which might be of interest. These include compounds such as  $\text{Pb}_2(\text{RE})\text{MoO}_6$ ,  $\text{Na}(\text{RE})(\text{MoO}_4)_2$ , and others. (For Pb and Na in these formulas, some alkaline earth or other alkali metal, respectively, might be substituted.) Very little is known of such compounds, though,<sup>23</sup> and considerable preliminary investigation will be necessary before a decision to prepare any of them can be made. (The sodium rare-earth molybdates appear to be paramagnetic and centrosymmetric, so some modification would obviously have to be introduced there.) Other types of materials containing rare earths and 3d-ions, principally niobates and borates, are also being looked into.

## NARROW-GAP AND NARROW-BAND COMPOUNDS

### Introduction

There is a great deal of interest at present in materials which undergo transitions from a semiconducting or insulating state to a metallic one. Such transitions occur with changes in temperature or pressure, and also possibly with applied electric field, although this has never been unambiguously confirmed. Such an electric-field-induced transition might be of great practical value. While the understanding of these transitions as a general phenomenon is at best rudimentary, the difficulties, both experimental and theoretical, being formidable, it appears that many transitions involve the formation, from what were localized states, of some sort of (probably) narrow conduction band. It appears that some samarium compounds, where low-lying excited states may be just localized, are among the most interesting materials of this type.<sup>24</sup> Of particular importance for initial studies because of the gradual low-activation-energy transition it shows at low temperature is samarium hexaboride,<sup>25</sup>  $\text{SmB}_6$ . It was at first thought that the transition in this material simply reflected a gradual valence change of  $\text{Sm}^{2+}$  to  $\text{Sm}^{3+}$  with increasing temperature. Subsequently, Mossbauer measurements<sup>26</sup> were interpreted as showing that both divalent and trivalent ions were present in a proportion independent of the temperature. A model of activation of localized excited states was proposed. More recently, results on Sm chalcogenides<sup>24</sup> have revived the divalent-trivalent picture somewhat. It seemed to us that the situation could be clarified by i) resistivity measurements on single crystals of  $\text{SmB}_6$ , rather than the powders previously used and ii) electron spin resonance studies to determine the valence state of the Sm ion. Also it seems that  $\text{SmB}_6$  might be a good material in which to look for an electric-field-induced transition.

### Preparation

$\text{SmB}_6$  was prepared in powder form by reacting intimate mixtures of  $\text{Sm}_2\text{O}_3$  and  $\text{B}_4\text{C}$  in dynamic vacuum. The reactants were mixed and ground together

and were slowly rf-heated in a Ta susceptor-container in vacuo to 1500 C and held for several hours. These steps were then repeated to ensure complete reaction. The reaction presumably is  $\text{Sm}_2\text{O}_3 + 3\text{B}_4\text{C} \rightarrow 2\text{SmB}_6 + 3\text{CO}\uparrow$ . Initial preparations were made with 99.9%  $\text{Sm}_2\text{O}_3$ . Subsequently, preparations were made with 99.99%  $\text{Sm}_2\text{O}_3$ .

The  $\text{SmB}_6$  powder was hydrostatically pressed at 6 kbar; then sintered at 1500 - 1900 C for 0.5 to 2 hours. The sintered slugs were still porous, with porosity estimated at about 10% in the better cases.

The slugs were used as feed material for melt-growth of the compound. They were placed in a water-cooled Cu boat in a hydrogen or helium atmosphere and were melted by use of a 4 MHz rf field. In the course of the melting, some material vaporized from the melt and deposited on adjacent cooler portions of the system. This material could not easily be identified by X-ray diffraction analysis since it was amorphous. However, emission spectrography showed that the vaporized material contained major concentrations of both samarium and boron. In connection with the melting of one specimen of hexaboride which contained a minor phase of  $\text{SmB}_4$ , the results of X-ray diffraction analysis before and after melting revealed that the concentration of  $\text{SmB}_4$  was decreased appreciably by the melting. Thus, it appears that composition tends to remain near  $\text{SmB}_6$  during the high-temperature processing.

It has been possible to obtain sizable (i.e., dimensions up to 1 cm) sound pieces of  $\text{SmB}_6$  by rf melting. Material melted in hydrogen was found to contain bubble-like voids, presumably due to the dissolution of hydrogen in the molten material and its exsolution as freezing occurs. Material melted in helium, however, has been void free and found to contain relatively large crystals (up to 4 mm<sup>2</sup> faces), revealed by cleavage. In further planned preparation work, attempts will be made to increase ingot size and to zone melt or directionally freeze the  $\text{SmB}_6$ .

#### Physical Measurements

Two basic measurements have been made so far on  $\text{SmB}_6$ . These are DC electrical conductivity and electron spin resonance.

Two samples of  $\text{SmB}_6$  were used for measurement of electrical transport properties. One was obtained from the initial pressed and sintered ingot and one from a fused ingot. As discussed above, there were substantial differences in porosity, density, and hardness and rather smaller differences in composition between the two types of specimens. The sintered specimen was rather porous and soft, but was single phase. The fused specimen, on the other hand, was hard and dense but contained  $\text{SmB}_4$  in trace amounts.

As a result of the high porosity in the one case, and the presence of  $\text{SmB}_4$  in the other, neither sample was of the superior quality desired for meaningful evaluation of detailed electrical measurements.

Nonetheless, resistivity data were obtained on both specimens at 300 and 77 K. The results are presented below:

| <u>Sample</u> | <u>Resistivity <math>\rho</math>, ohm-cm</u> | <u>Temperature, <math>^{\circ}\text{K}</math></u> | <u><math>\rho_{77}/\rho_{300}</math></u> |
|---------------|--|---|--|
| Sintered      | $7.13 \times 10^{-4}$                        | 300   | 1.20                                     |
|               | $8.58 \times 10^{-4}$                        | 77  |  |
| Fused         | $6.37 \times 10^{-4}$                        | 300   | 1.42                                     |
|               | $9.05 \times 10^{-4}$                        | 77  |  |

Based on this data, both specimens appear to be semiconducting. The resistivity ratio is higher in the fused specimen and also appears a little higher than that reported by Menth et al.<sup>25</sup> It is not known at this time whether the difference between our samples is the result of voids, crystalline perfection, variation of composition, or impurities. Resolution of these questions awaits preparation of still better samples.

As mentioned above, it has been proposed that the mechanism for conduction in  $\text{SmB}_6$  is the delocalization of a 4f electron of the  $\text{Sm}^{2+}$  ( $4f^6$  configuration) by thermal excitation to the 5d conduction band. Mossbauer experiments<sup>26</sup> were interpreted in terms of the presence of both  $\text{Sm}^{2+}$  and  $\text{Sm}^{3+}$ , but no changes in the spectrum were observed as the temperature was varied through the transition region. In addition, magnetic susceptibility measurements have been unsuccessful in detecting the expected paramagnetism of the  $\text{Sm}^{3+}$  ion. We began



a series of EPR experiments to determine the valence state of the Sm ion.  $\text{Sm}^{2+}$  has a  $J = 0$  ground state and is thus not magnetic, while  $\text{Sm}^{3+}$  has  $J = 5/2$ . We have observed a very broad resonance in the  $\text{SmB}_6$  sample, but its effective gyromagnetic ratio is not commensurate with that expected for a  $\text{Sm}^{3+}$  ion in a crystal field appropriate to the  $\text{SmB}_6$  lattice. Since the first excited angular momentum state ( $J = 1$ ) of the  $\text{Sm}^{2+}$  ion is only about 380 K above the ground state it is conceivable that the observed resonance is due to this state. The resonance is very broad, as might be expected if the lifetime of the excited state is short, and shows an intensity variation with temperature which is roughly commensurate with the Boltzmann distribution. To our knowledge the EPR of a thermally excited angular momentum state has never been reported. We are therefore attempting to observe this effect in other systems where the Sm ion is known to be divalent and we are considering appropriate distortions of cubic crystalline field which would predict the observed gyromagnetic ratio.

The direction of work in the near future should be clear from the foregoing. Eventually we hope to look at some other narrow-gap compounds in which samarium is normally divalent; as mentioned below,  $\text{Sm}_2\text{As}_3$  (which does not seem ever to have been prepared) is one such possibility. We also wish to mention that some time in the next year we hope to have available results of band structure calculations (being carried out on a Battelle-sponsored project) on the samarium monochalcogenides which should be helpful in interpretation of some data.

PNICTIDES

## Introduction

The rare-earth monpnictides are compounds of formula (RE)(Pn) where Pn denotes one of the so-called pnigogens - N, P, As, Sb or Bi. Almost all of these compounds have the simple NaCl structure. The nature of these materials--whether they are semiconducting or metallic, or whether they are inherently non-stoichiometric--has been a subject of investigation and controversy for the past ten years. In the past year or so, however, a good deal of experimental evidence has been presented which is interpreted as showing that these materials are all metallic (or perhaps semi-metallic, though it is hard to see how this could be). The evidence is relatively clear in the phosphides, arsenides, antimonides and bismuthides, where there are fewer problems with stoichiometry and where there are (in the first three cases) recent nuclear magnetic resonance measurements<sup>27</sup> which indicate a hyperfine field more typical of a metal. The situation is not nearly so unambiguous in the nitrides, where stoichiometry is very difficult (perhaps impossible) to attain. Briefly stated, and omitting references, the principal arguments one might advance that the rare-earth nitrides should be semiconductors are as follows:

- 1) Band calculations on ScN indicate that it is semiconducting or semimetallic, and introduction of f-levels should push the valence and conduction bands further apart,
- 2) There is evidence in the optical absorption of something resembling an energy gap,
- 3) Large crystal field effects are apparent in magnetic properties of some nitrides,
- 4) Metallographic examination of some nitrides shows a tendency for metal to concentrate at grain boundaries.

Likewise, the principal arguments for metallic character of these compounds are:

- 1) Transport property measurements are generally typical of metals,
- 2) Specific heat and photoemission measurements can be interpreted as indicating a considerable density of electrons at the Fermi surface,
- 3) Changes in magnetic properties on adding small amounts of oxygen or carbon are of the sort expected in a metal.

Objections can easily be raised to all the evidence on both sides. For instance, the plausibility of interpreting large crystal field effects as indicative of high ionicity, and thus of semiconductivity, is considerably lessened by the observation that in hexaborides doped with rare earths, crystal field effects on the dopant ions are clearly larger in the metallic than in the semiconducting materials<sup>28</sup>.

When we undertook work to understand something of the nature of these materials, we thought of transport measurements on sound materials (previous measurements are on pressed powders) of as near stoichiometric composition as possible. A little reflection shows that this is not necessarily such a good idea, since one has no way of knowing how near stoichiometry is near enough. What is more, it may well be that difficulty in obtaining sound samples is not independent of the difficulty in achieving stoichiometry (such is the case in some III-IV semiconductors), and to the extent that non-stoichiometry is intrinsic, compact homogeneous samples of reasonable size might prove extremely difficult to produce. In view of this, it seems more reasonable to undertake nuclear magnetic resonance measurements on samples as near stoichiometry as possible, but with known deviations therefrom. Difficulties with unsound samples may thus be turned into assets, provided only that the samples are reasonably homogeneous. Some previous NMR measurements<sup>29</sup> on TbN and TmN, while not particularly conclusive, are encouraging in that they indicate that the nitrogen resonance is observable. Our measurements should start soon, awaiting only the preparation and characterization of somewhat larger quantities of GdN, the nitride previously selected for initial study.

## Preparation

In work by others, rare-earth nitrides have been prepared by arc melting<sup>30</sup> and by "flash" melting<sup>31</sup> in nitrogen atmospheres and by reaction between the rare-earth hydrides and ammonia<sup>32</sup>. In all cases for which analytical data have been presented, the material was found to be nitrogen deficient, with deficiencies ranging from a few tenths percent (concluded indirectly) to 10%. In one investigation<sup>33</sup>, films were formed by vacuum evaporation. However, the films were kept in high vacuum and no analysis or characterization was made of the film material other than that of optical transmission. In all other investigations for which material preparation has been described, powder material was pressed and sintered to obtain bulk specimens for study.

The objective of synthesis work on this program has been the development of techniques for the direct preparation of bulk specimens, thus circumventing the need for the pressing and sintering step and avoiding its deficiencies. GdN was selected as the principal pilot material and the reactions of ammonia and nitrogen with Gd metal in bulk form have been investigated. For the ammonia - metal reaction, temperatures in the range 1065 C to 1115 C and a gas flow system were employed. When initial results indicated the possibility of water in the ammonia, a calcium oxide drying column was added to the flow train to dry the ammonia. Although GdN was produced by this reaction, oxide always was present - usually as an outer layer - and it did not appear that oxide-free material could be produced readily in the ammonia flow system.

Subsequent preparations have utilized the Gd metal - nitrogen reaction. Reaction temperatures have been around 1500 C. Temperature was brought up slowly to 1500 C, and dry nitrogen distilled from a liquid nitrogen reservoir was employed. Results indicate that bulk GdN samples can be prepared by such reaction at moderate temperatures in this range. Most runs so far have only been partially successful because of equipment failures producing catastrophic temperature increases. At the other extreme, when the reaction rate is held down (by use of low reaction temperature) a surface layer of oxide is observed to form--presumably due to diffusion of oxidic species through tubing connections of the

reactor in the course of the long reaction run. Plans call for continued work on direct synthesis using completely sealed silica reaction ampoules.

#### Discussion

It is reasonable to inquire whether measurements on a single nitride would be sufficient to ascertain the nature of the conductivity in all the rare-earth nitrides (beyond Pr). If one is willing to accept the premise that changes in degree of ionicity generally will be reflected in changes in lattice parameter, some pertinent information can be obtained just from studying the published lattice parameter data. A non-metaphysical way to do this<sup>33</sup> is to plot the parameters for the rare-earth nitrides against the corresponding data for the trivalent sulfides. One finds on doing this that the plotted points fall rather closely on a straight line, which may be taken as an indication that the degree of ionicity, and hence probably the conduction mechanism, is similar in all the rare-earth nitrides. The point for dysprosium falls a little below the line, but probably not far enough to be significant.

Our immediate plans for future work have already been described. If, as seems possible, the rare-earth mononitrides appear really to be metallic and/or to be inherently non-stoichiometric, we will not abandon work on the pnictides altogether, but rather will look at compounds of the type  $(RE)_3(Pn)_2$ . In these compounds, those rare earths that can easily be divalent will probably assume that state, and the compounds will usually be narrow-gap semiconductors<sup>34</sup>.

### NON-RADIATIVE ENERGY TRANSFER AMONG RARE-EARTH IONS

The fluorescence properties of rare-earth ions present as dopants in dielectric crystals are of importance in the design of devices such as lasers and infrared-to-visible frequency converters. The spectroscopic properties of isolated rare-earth ions in many hosts are well known. However, the quantum efficiency and decay times of particular fluorescent states can be influenced by the presence of other rare-earth ions in the crystal. In addition, interactions between ions may result in new fluorescence excitation schemes. Although there has been some investigation of nonradiative transfer of energy and of cooperative interactions among rare-earth ions<sup>35</sup>, this is an area in which there is still much to be learned. Therefore, a series of experiments was undertaken which was directed toward increasing our understanding of a particular example of cooperative excitation, namely, the infrared excitation of red fluorescence in  $\text{Ho}^{3+}$ , present as a dopant in  $\text{CaF}_2$ .

The initial experiments were steady-state measurements of the red fluorescence output as a function of the infrared input. These established that two IR photons were involved in the production of each red photon. Additional steady-state measurements of the output as a function of  $\text{Ho}^{3+}$  concentration indicated that, on the average, more than one ion was involved in each emission event. This situation was clarified after we developed a dynamic theory for the cooperative process. Comparison of this theory with experimental data taken on a pulsed basis established that two ions were involved in each event.

The explanation of the process by which the fluorescence was excited is that two ions, each excited to the  $^5\text{I}_6$  level, cooperate in the transfer of excitation from one ion to the other, with the result that one ion is further excited to the  $^5\text{F}_5$  level and the other deexcited to the ground state. Examination of the energy level diagram (Fig. 7) shows that the energy of the  $^5\text{F}_5$  level is considerably less than twice that of the  $^5\text{I}_6$  level. Furthermore there is no single-ion excited state with this energy. This means that

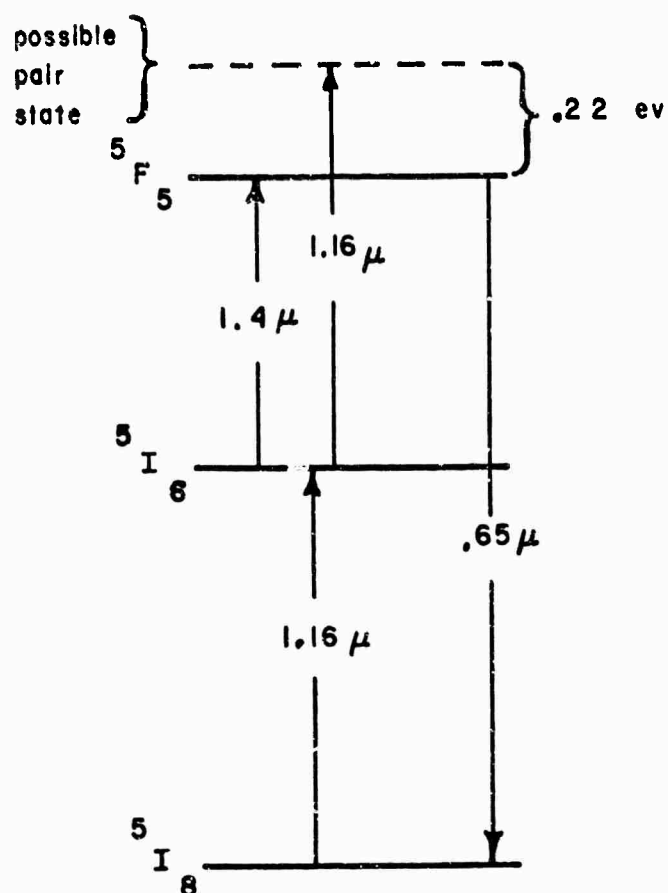


FIGURE 7. PARTIAL ENERGY LEVEL DIAGRAM OF  $\text{Ho}^{3+}$  IN  $\text{CaF}_2$ , SHOWING ENERGY MISMATCH IN THE COOPERATIVE PROCESS.

there is an apparent lack of conservation of energy in this process which we felt had to indicate the emission of phonon into the crystal lattice. The probability of this type of event is a strong function of the number of phonons involved. The  $\text{CaF}_2$  lattice will support relatively energetic phonons compared to  $\text{LaF}_3$  which has a much lower Debye temperature. To verify the participation of the lattice in the cooperative event, the cooperative excitation experiment was attempted in  $\text{LaF}_3$ . No red output could be seen, thus confirming the notion that the lattice must participate in the cooperative excitation process. This work has been submitted for publication.

Further work will provide a more detailed understanding of the cooperative excitation process. Previous theories of the process assume an interaction constant for the transfer of energy from one ion to another which has no explicit dependence upon the distance between ions. This is an obviously unrealistic condition which can be avoided by assuming that the interaction has such a strong radial dependence that only neighbor ions can take part in the cooperative event. This model leads to results which agree with experimental data. If these near-neighbor pairs interact strongly enough, then they ought to form pair states which will have absorption spectra with characteristics which are different from those of the isolated ion. We plan to look for these spectroscopic features. In addition, the role of the lattice will be considered in more detail. A particular experiment which will aid in this is the temperature dependence of the efficiency of the cooperative interaction. This will show whether the lattice merely acts as a sink for phonons or whether the transition from the pair state to the single-ion state is stimulated by the presence of phonons in the crystal.



## REFERENCES

1. A. R. Billings, Tensor Properties of Materials (Wiley-Interscience, 1970);  
R. R. Birss, Symmetry and Magnetism, (North-Holland, 1964);  
R. M. Hornreich, Solid State Communs. 7, 1081 (1969).
2. N. N. Neronova and N. V. Belov, Soviet Phys. - Crystallog. 4, 769 (1960);  
V. N. Lyubimov, Soviet Phys. - Crystallog. 10, 433 (1966);  
A. E. Austin, Battelle-Columbus internal report (1968) (copies available).
3. W. F. Brown, Jr. et al, Phys. Rev. 168, 574 (1968).
4. Yu. A. Gufan, JETP Letters 8, 167 (1968).
5. R. Pauthenet and C. Veyret, J. de Physique 31, 65 (1970).
6. F. Bertaut, F. Forrat, and P. Fang, Comptes Rendus 256, 1958 (1963).
7. A. Waintal and J. Chenavas, Mat. Res. Bull. 2, 819 (1967); Comptes Rendus 264, 168 (1967).
8. H. L. Yakel et al., Acta Cryst. 15, 957 (1963).
9. A. P. Young, P. B. Robbins, and C. M. Schwartz, High Pressure Measurements,  
(A. A. Giardini and E. C. Lloyd, Eds.) 262 (Butterworths, Washington, (1963));  
P. N. LaMori, Ibid, 321 (1963).
10. J. E. Mee et al., IEEE Trans. Mag. 5, 717 (1965).
11. F. H. Wehmeier, J. Crystal Growth 6, 341 (1970).
12. R. Buhl, J. Phys. Chem. Solids 30, 805 (1969).
13. K. Dwight and N. Menyuk, Phys. Rev. 119, 1470 (1960).
14. C. N. R. Rao and G. V. Subba Rao, Proc. 8th Rare-Earth Research Conference  
(Reno, 1970) 653.
15. I. G. Ismailzade and S. A. Kizhaev, Sov. Phys. - Solid State 7, 236 (1965).
16. G. V. Subba Rao et al., Solid State Communs. 6, 177 (1968).

17. K. Kritayakirana et al., Optics Communs. 1, 95 (1969).
18. H. J. Borchardt and P. E. Bierstedt, J. Appl. Phys. 38, 2057 (1967);  
L. E. Cross et al, Phys. Rev. Letters 21, 812 (1968).
19. E. T. Keve et al., Solid State Communs. 8, 1517 (1970), and private communication.
20. L. A. Drobyshev et al., Sov. Phys. - Crystallog. 13, 964 (1969); 15, 53 (1970).
21. J. Kvapil and V. John, Phys. Stat. Sol. 39, K15 (1970).
22. S. E. Cummins, Ferroelectrics 1, 11 (1970);  
K. Aizu et al., J. Phys. Soc. Japan 27, 511 (1969).
23. G. A. Smolensky et al., Proc. Internat. Cong. Magnetism (Nottingham, 1964) p. 354;  
C. D. Brandle and H. Steinfink, Proc. 8th Rare Earth Research Conf. (Reno, 1970), p. 235;  
L. Holmes and M. Schieber, J. Phys. Chem. Solids 29, 1663 (1968).
24. A. Jayaraman et al., Phys. Rev. Letters 25, 368, 1430 (1970).
25. A. Menth et al., Phys. Rev. Letters 22, 295 (1969).
26. R. L. Cohen et al., Phys. Rev. Letters 24, 383 (1970).
27. E. D. Jones, Phys. Rev. 180, 455 (1969).
28. Z. Fisk, Phys. Letters 30A, 152 (1969).
29. R. G. Shulman and B. J. Wyluda, J. Phys. Chem. Solids 23, 166 (1962).
30. N. Sclar, J. Appl. Phys. 35, 1534 (1964).
31. R. J. Gambino and T. R. McGuire, J. Appl. Phys. 41, 933 (1970).
32. M. K. Wilkinson et al., J. Appl. Phys. 31 358S (1960);  
R. Didchenko and F. P. Gortsema, J. Phys. Chem. Solids 24, 863 (1963);  
F. Anselin, Comptes Rendus 256, 2616 (1963).

33. F. Hulliger, *Helv. Phys. Acta* 41, 945 (1968).
34. F. Hulliger and O. Vogt, *Solid State Commun.* 8, 771 (1970).
35. V. V. Ovsyankin and P. P. Feofilov, *JETP Letters* 3, 322 (1966).

## DOCUMENT CONTROL DATA - R &amp; D

(Security classification of title, body of abstract and indexing annotation must be entered when the overall report is classified)

|  |   |  |  |
|--|---|--|--|
| 1. ORIGINATING ACTIVITY (Corporate author)<br>Battelle Memorial Institute, Columbus Laboratories<br>505 King Avenue<br>Columbus, Ohio 43201  |   | 2a. REPORT SECURITY CLASSIFICATION<br>UNCLASSIFIED   |  |
|  |   | 2b. GROUP  |  |
| 3. REPORT TITLE<br><br>PREPARATION AND PROPERTIES OF RARE-EARTH COMPOUNDS  |   |  |  |
| 4. DESCRIPTIVE NOTES (Type of report and inclusive dates)<br>Semi-Annual Technical Report (4 June 1970 to 4 December 1970)   |   |  |  |
| 5. AUTHOR(S) (First name, middle initial, last name)<br>V. E. Wood, K. C. Brog, A. E. Austin, J. F. Miller, W. H. Jones, Jr., C. M. Verber,<br>E. W. Collings, R. D. Baxter  |   |  |  |
| 6. REPORT DATE<br>December 31, 1970  | 7a. TOTAL NO. OF PAGES<br>38  | 7b. NO. OF REFS<br>35  |  |
| 8a. CONTRACT OR GRANT NO.<br>DAAH01-70-C-1076  | 9a. ORIGINATOR'S REPORT NUMBER(S)<br>Battelle Project G-0550                |  |  |
| b. PROJECT NO.   |   |  |  |
| c.   | 9b. OTHER REPORT NO(S) (Any other numbers that may be assigned this report) |  |  |
| d.   |   |  |  |
| 10. DISTRIBUTION STATEMENT<br>Distribution of this document is unlimited.  |   |  |  |
| 11. SUPPLEMENTARY NOTES  |   | 12. SPONSORING MILITARY ACTIVITY<br>Advanced Research Projects Agency<br>Arlington, Virginia 22209 |  |
| 13. ABSTRACT<br>Research has been performed to investigate potentially useful properties of rare-earth materials, including studies in the areas of magnetoferroelectricity, narrow-band and narrow-gap compounds, rare-earth pnictides, and cooperative fluorescence of rare-earth ions in crystals. Manganates of Dy, Y, Ho, and Yb (including high-pressure orthorhombic phases of the last three) and molybdates of Eu, Gd, and Tb have been prepared and their electrical and magnetic properties studied. Although some of these compounds have interesting magnetic transitions, none appears to be even weakly ferromagnetic above about 10 K and hence they are not particularly attractive as ferro-magneto-ferroelectrics. Electron paramagnetic resonance studies of the gradual low-temperature semiconductor-to-metal transition in $\text{SmB}_6$ show a resonance which tentatively has been attributed to an excited state of $\text{Sm}^{2+}$ . Transport measurements on a recently prepared high-purity, rf-melted sample of $\text{SmB}_6$ will be made shortly. Results of both studies should provide insight into the conduction mechanism and the nature of the transition in such materials. Though recently reported research indicates that all rare-earth monopnictides ((RE)Pn; Pn = N, P, As, Sb, or Bi with NaCl structure) are metallic, this may be due to intrinsic non-stoichiometry, and the question of whether the nitrides, in particular, are "really" metallic or semiconducting must still be considered open. Samples of $\text{GdN}$ have been prepared and nuclear magnetic resonance studies will be used to determine the role of defects and to try to elucidate the electronic character. Finally, studies on the two-photon infrared-excited red fluorescence of $\text{Ho}^{3+}$ ions in $\text{CaF}_2$ have established that the fluorescence arises from cooperative energy transfer between $\text{Ho}^{3+}$ ions rather than from successive excitation of a single ion. Work is continuing to determine the exact mechanism of the cooperative process. |   |  |  |

| 14<br>KEY WORDS  | LINK A |    | LINK B |    | LINK C |    |
|--|--------|----|--------|----|--------|----|
|  | ROLE   | WT | ROLE   | WT | ROLE   | WT |
| Magnetoferroelectric Materials<br>Semiconducting Compounds<br>Semiconductor-to-metal transitions<br>Rare-earth manganates<br>Rare-earth molybdates<br>Rare-earth borides<br>Rare-earth nitrides<br>Cooperative luminescence<br>$\text{CaF}_2:\text{Ho}^{3+}$ |        |    |        |    |        |    |